Self-assembly of organic films on a liquid metal

Olaf M. Magnussen*†, Benjamin M. Ocko*, Moshe Deutsch‡, Michael J. Regan§, Peter S. Pershan§, Douglas Abernathy||, Gerhard Grübel|| & Jean-François Legrand||¶

* Physics Department, Brookhaven National Laboratory, Upton, New York 11973, USA
‡ Physics Department, Bar-Ilan University, Ramat-Gan 52100, Israel
§ Division of Applied Science & Physics Department, Harvard University, Cambridge, Massachusetts 02138, USA
|| European Synchrotron Radiation Facility, BP 220, 38041 Grenoble Cedex, France
¶ Laboratoire de Spectrometrie Physique, UJF, BP 53, 38403 Grenoble Cedex, France

THE structure and phase behaviour of organic thin films result from the subtle interplay of intermolecular Van der Waals interactions, which promote self-assembly and long-ranged order, and the more complex interactions between the end groups of the organic chains and the substrate. The structure of molecular films of amphiphiles has been extensively studied on subphases of dielectric liquids, notably water (Langmuir monolayers) and on solid surfaces (self-assembled monolayers, SAMs)[1–4]. Here we report structural studies, by synchrotron X-ray scattering, of an intermediate case: densely packed alkanethiol films on the surface of liquid mercury. While, like SAMs, these films form strong chemical bonds to the subphase, this subphase is smooth and unstructured, as in the case of Langmuir monolayers. But unlike either of these[1,2,5–7], our films have no in-plane long-range order. We suggest that the strong interaction of the thiol group with the underlying disordered liquid dominates here over the order-promoting interactions of the alkyl chains.

The significantly different structures of SAMs and Langmuir monolayers composed of similar chain-like molecules reflect fundamental differences in the subphase–end-group interactions. First, the bond strengths of SAMs to solid substrates (typically a few hundred kilojoules per mole) greatly exceed those of the typical hydrogen bonds of Langmuir monolayers to water or organic subphases ($\leqslant 10\,\mathrm{kJ\,mol^{-1}}$)[8]. Second, the liquid subphase molecules can rearrange freely and lack intrinsic in-plane order, whereas the crystalline SAM substrates possess well defined long-range order. Accordingly, the order in alkanethiols on crystalline gold, the best-studied SAM[3], is induced epitaxially by the strong ($418\,\mathrm{kJ\,mol^{-1}}$)[9] Au–S bond. Even the corrugation potential, the 5–20% spatial modulation of the binding energy induced by the substrate's periodic structure, still exceeds considerably the inter-chain interactions of the alkylthiols ($\leqslant 1\,\mathrm{kJ\,mol^{-1}}$ per CH_2 unit)[8]. In Langmuir monolayers, by contrast, the order is induced by inter-chain interactions, which exceed the hydrogen-bond strength in molecules longer than 10–15 carbons.

Alkanethiols on liquid mercury provide a system which can, in principle, help to disentangle the influence of adsorbate–substrate bond strength from the lattice periodicity. The liquid mercury surface lacks long-range order, while the Hg–S binding energy ($\sim 200\,\mathrm{kJ\,mol^{-1}}$)[9] is comparable to those of Au–S, Ag–S and Cu–S ($200–400\,\mathrm{kJ\,mol^{-1}}$)[9] and is over ten times stronger than the hydrogen bonds of Langmuir monolayers. Unlike their solid counterparts, the ultra-smooth liquid metal subphases are free from any static structural surface features like corrugations, atomic steps and defects. Much thermodynamic and kinetic data exists for organic films on mercury (both at the vapour[10] and electrochemical interfaces[11,12]), but no direct structural information has previously been available.

† Present address: Universität Ulm, Abt. Oberflächenchemie und Katalyse, 89069 Ulm, Germany.

We have investigated alkanethiols, $CH_3(CH_2)_{n-1}SH$ (denoted C_n) with $n = 8$, 12, 16, 18, 22 and 30 on clean liquid mercury surfaces by grazing-incidence X-ray diffraction (GIXD), a technique sensitive to the molecular structure within the surface plane, and X-ray reflectivity, which probes the surface-normal electronic density profile. Both techniques have been applied recently to studies of the clean surfaces of liquid mercury[13,14] and liquid gallium[15], revealing a liquid-like in-plane arrangement of the surface atoms[14], atomic stratification in the surface normal direction and sub-ångström roughness[13,15]. $R(q_z)$, the measured reflectivity profile for wavevector q_z of the liquid mercury surface covered by C_{18} is shown in Fig. 1 (circles). The data closely follow the reflectivity R_{Hg} of clean liquid mercury at low q_z and both are only slightly lower than the Fresnel reflectivity R_f of an ideally flat surface. This indicates a similar, small surface roughness for the bare and thiol-covered mercury surfaces. At $q_z > 0.5\,\text{Å}^{-1}$, R dips significantly below R_{Hg} but approaches it again at the broad peak around $2.16\,\text{Å}^{-1}$. As this peak characterizes the atomic surface layering of the mercury subphase[13], its persistence for the thiol-covered surface indicates that the organic film induces no major changes in the liquid-metal surface structure. The most significant change, compared with the bare mercury surface, is the emergence of periodic oscillations.

The Fresnel-normalized reflectivity (Fig. 2) further highlights these features. The period of the five oscillations observed in Fig. 2*a*, $\Delta q_z \approx 0.25\,\text{Å}^{-1}$, corresponds to a layer thickness $d = 2\pi/\Delta q_z = 25\,\text{Å}$, in agreement with the length of a fully extended C_{18} molecule. Similar features are observed for thiols of different lengths n. For example, R/R_f of the C_{12} monolayer (Fig. 2*b*) has a very similar overall shape to Fig. 2*a* but the oscillation

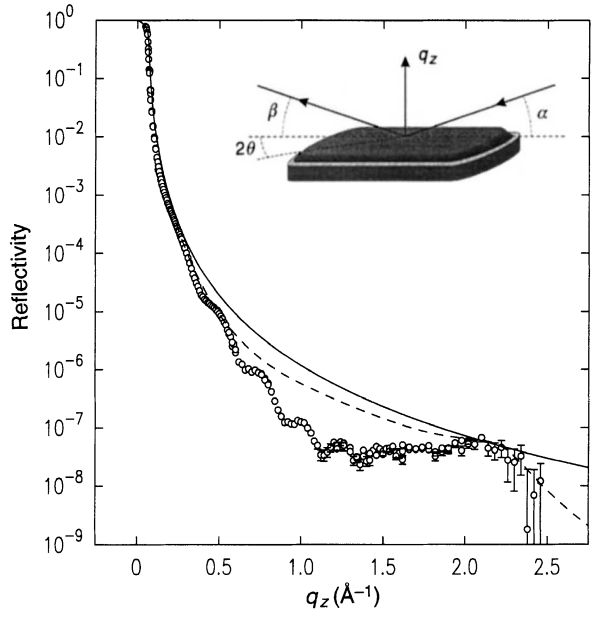

FIG. 1 X-ray reflectivity from a C_{18} ($CH_3(CH_2)_{17}SH$) monolayer-covered (circles) and a bare (dashed line) liquid mercury surface. The Fresnel reflectivity R_f (solid line) is also shown. The presence of the monolayer is clearly indicated by the oscillatory modulations of the reflectivity. The inset shows the experimental geometry. Alkanethiols were deposited by direct application of the thiols in their liquid state, by chemical vapour deposition, by self-assembly from an ethanol bath, or by spreading from a dilute chloroform solution. All techniques yielded well defined monolayers. X-ray reflectivity measurements (at wavelengths $0.65\,\text{Å} \leqslant \lambda \leqslant 1.2\,\text{Å}$) were carried out at beamline X22B[13] and wiggler beamline X25[15] at the National Synchrotron Light Source (Brookhaven) at room temperature and under nitrogen. Exposure to the beam was minimized to avoid beam damage. The absolute reflectivity was obtained from measurements along the specular axis ($2\theta = 0°$), subtracted by the diffuse background (measured at $2\theta = \pm 0.6°$) and normalized to the direct beam intensity.

period is increased to $\Delta q_z = 0.36\,\text{Å}^{-1}$, corresponding to the shorter length of this molecule $d = 2\pi/\Delta q_z = 17.5\,\text{Å}$. Oscillations which scale with the length of the C_n molecule have been observed for all thiols studied ($8 \leqslant n \leqslant 30$), demonstrating a very similar monolayer structure for all lengths. For long chains ($n = 22, 30$), however, the oscillations are weak and the reflectivity data indicates a high interfacial roughness.

Quantitative information on the atomic arrangement along the surface-normal direction is obtained by fitting the reflectivity data to a density-dependent model reflectivity calculated from the Born approximation[16]. The fitted profiles, displayed as solid lines in Fig. 2 with identical parameters for all data sets (apart from the number of CH_2 groups), are in excellent agreement with the experimental data. The corresponding density profiles are shown in Fig. 3. Comparison with the density profile for the clean mercury surface reveals the extended hydrocarbon tail, and the higher-density sulphur atom between the mercury and the hydrocarbon tail. The slight decrease observed in the amplitudes of the first mercury layers probably reflects the small increase in surface roughness expected by the capillary-wave model from a decrease in the surface tension due to the monolayer's presence. Despite this, the general features of a layered mercury surface with an adsorbed, densely packed monolayer of fully extended molecules are found in all the systems studied. Also, the surface roughness (estimated from the density profile width of the first mercury layer) remains about 1 Å, that is, in good agreement with the value given by capillary-wave theory[13].

Because of the high adlayer density ($0.34 \pm 0.02\,\text{e Å}^{-3}$), which is close to that found in crystalline alkanes and significantly higher than in the melt, in-plane ordering of the molecules might be expected. Despite an exhaustive search at two of the most intense beamlines worldwide, no sharp in-plane peaks corresponding to an ordered adlayer structure were found for the monolayer phases of thiol molecules of any of the examined lengths. In particular, a careful search was done from 1.5 to $1.7\,\text{Å}^{-1}$ where structurally similar SAMs and Langmuir monolayers show the lowest-order in-plane peaks. The GIXD data is shown in Fig. 4 for the clean and C_{18}-covered mercury surface. Both show the characteristic broad peaks around the in-plane wavevectors $q_{\|} \approx 2.3\,\text{Å}^{-1}$ and $q_{\|} \approx 4.5\,\text{Å}^{-1}$ expected for liquid mercury[14] although at different relative intensities, which may indicate a thiol-induced modification of the mercury surface structure. As we discuss below, the absence of in-plane order in the densely packed alkanethiol monolayer is probably promoted by the disordered mercury subphase via the strong, covalent Hg–S bond. We note that at thiol coverages greater than a monolayer, sharp, resolution-limited in-plane peaks are readily observed, corresponding to the formation of well-ordered multilayer phases (O.M.M. *et al.*, manuscript in preparation).

The results presented here highlight the importance of the relative strengths of the substrate–end-group and inter-chain interactions and the specific order preferred by each. In systems where the latter dominate, such as densely packed films of alkanes, alcohols and fatty acids on pure water[1,2,17], long-range,

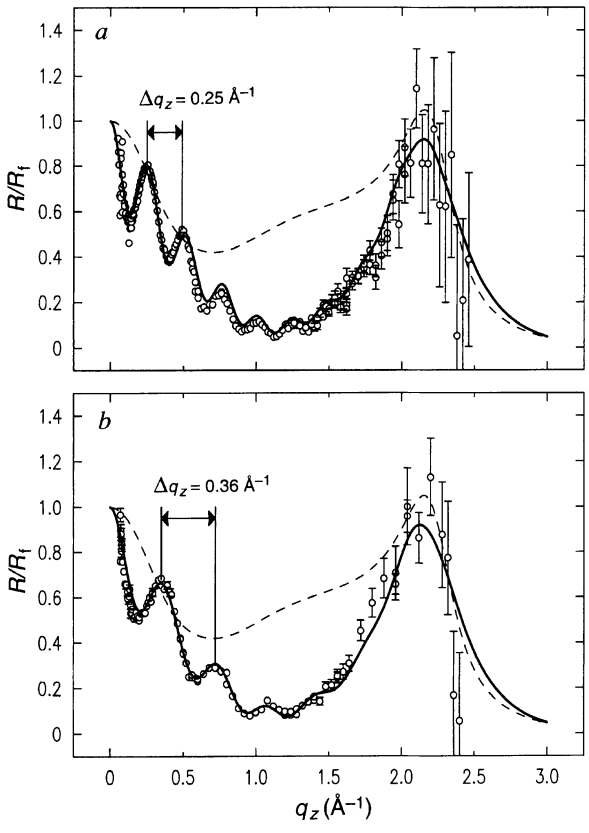

FIG. 2 The measured normalized reflectivity R/R_f of C_{18} (*a*) and C_{12} (*b*) monolayers on liquid mercury (circles) and of the bare mercury surface[13] (dashed line). The different periodicities Δq_z for C_{18} and C_{12} are indicated. Solid lines are fits to a model used to describe the atomic layering at the bare mercury surface[13], modified by adding $n + 1$ gaussians representing the n carbon units and the terminal sulphur, respectively. The area per molecule of the thiols was fixed at that of the high-coverage multilayer phase (19.23 Å^2 according to the GIXD diffraction pattern). The fits in *a* and *b* differ only in the number of CH_2 groups.

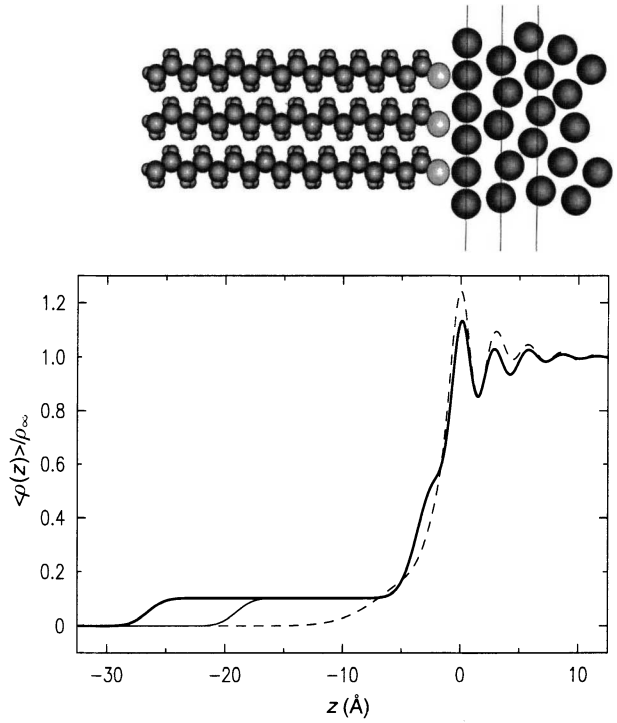

FIG. 3 Schematic real-space model and normalized electron density profiles $\langle\rho(z)\rangle/\rho_\infty$ (where ρ_∞ is the bulk electron density of mercury) obtained from the fits for C_{18} (bold line) and CH_{12} (thin line). The upper and lower figures are aligned with each other. Vertical lines in the model illustrate the position of the three outermost surface layers of mercury, with the origin of z coinciding with the first mercury layer. The carbon–carbon and the carbon–sulphur spacing along the surface normal were fixed at 1.25 and 1.5 Å, respectively. These spacings correspond to the projections of the carbon–carbon (1.53 Å) and the carbon–sulphur (1.82 Å) bonds onto the molecular axis. As the gaussian width describing the CH_2 groups (typically 1.2 Å) is considerably greater than half the separation between the carbon atoms, the density profile appears constant in the central part of the chain.

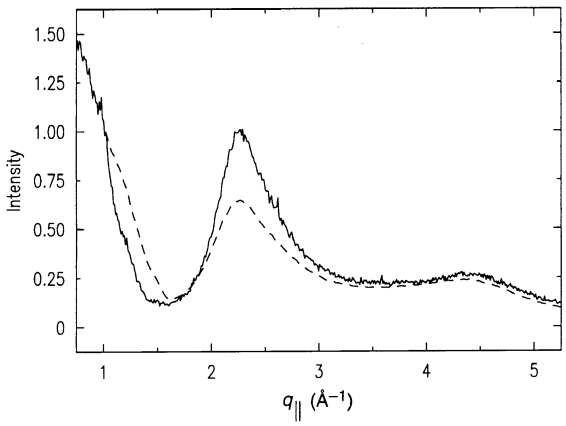

FIG. 4 Grazing-incidence diffraction patterns of a bare (dashed line) and a C_{18} monolayer-covered (bold solid line) mercury surface, measured with an incidence angle $\alpha = 0.2^\circ = 0.6\alpha_c$ (where α_c is the critical angle) and a vertical detector acceptance of $0 \leqslant q_z \leqslant 1.1\,\text{Å}^{-1}$ (intensity given in arbitrary units). Here $q_{||} = 4\pi/\lambda \sin\theta$ is the in-plane momentum transfer and θ is defined in Fig. 1 inset. Only the broad peaks corresponding to the mercury liquid structure factor are found in the monolayer data (in-plane resolution $\Delta(2\theta) = 5$ mrad). This data was obtained at the TROIKA undulator beamline of the ESRF[19]. GIXD measurements at X22B and X25 at NSLS gave similar results.

in-plane order is usually found. This order results not only from the confinement of the monolayer to the water surface, because such in-plane order also appears in alkanes where crystalline monolayers form at the surface of their own melts at temperatures up to a few degrees above the bulk freezing point[18]. In this case the 'monolayer' and 'subphase' molecules are identical, and, of course, fully miscible. Both systems are dominated by the inter-chain interactions and the bonds to the sub-phase ($\sim$10 kJ mol^{-1} hydrogen bonds in Langmuir monolayers and $\sim$1 kJ mol^{-1} van der Waals interactions in alkanes) are relatively weak. Thus, we conclude that the inter-chain interactions are responsible for the long-range order in these systems. The interactions with the disordered atoms of the liquid subphase tend, in principle, to disrupt this ordering but are too weak to cause more than slight changes in the structure and the phase diagrams of these films.

For SAMs, spatial variations of the interactions with the substrate (corrugation potential) may either promote or oppose the ordering favoured by the inter-chain interactions, depending on the spatial periodicities of both interactions. For alkanethiols on Au(111) (refs 5–7) this corrugation potential favours well ordered monolayers which may be either commensurate or uniaxial incommensurate with the underlying metal. The small mismatch between the underlying substrate and alkane spacings is compensated by a molecular tilt. The elevated melting temperature of C_n on Au(111) relative to that of the bulk[5] manifests the strong ordering tendency imposed by the interactions with the substrate.

Thiols on mercury 'feel' a similarly strong subphase interaction ($\sim$200 kJ mol^{-1}), but as the liquid mercury surface has no intrinsic long-range order, there is no underlying corrugation potential to order the thiol monolayer. This should promote formation of the order favoured by the inter-chain interaction. If, on the other hand, the ordered thiol layer were to impose its order on the underlying mercury through the strong subphase interaction, with the same structure as found for alkanethiols formed on gold and silver, then the resultant 5–10% compression of the mercury atoms would carry a great energy cost. In addition, this ordered mercury layer, at a temperature where the bulk is disordered, would represent a large increase in the entropic contribution to the free energy of the mercury and for these two reasons seems unlikely. Instead the (liquid-like) subphase surface structure is imposed on the adsorbate film, resulting in an in-plane-disordered film. □

Received 22 May; accepted 15 October 1996.

1. Knobler, C. M. *J. Phys.* **3,** 17–22 (1991).
2. Als-Nielsen, J., Jacquemain, D., Kjaer, D., Leveiller, F. & Leiserowitz, L. *Phys. Rep.* **246,** 252–313 (1994).
3. Ulman, A. *An Introduction to Ultrathin Organic Films: From Langmuir Blodgett to Self Assembly* (Academic, Boston, 1991).
4. Tredgold, R. H. *Order in Thin Organic Films* (Cambridge Univ. Press, 1994).
5. Fenter, P., Eisenberger, P. & Liang, K. S. *Phys. Rev. Lett.* **70,** 2447–2450 (1993).
6. Strong, L. & Whitesides, G. M. *Langmuir* **4,** 546–558 (1988).
7. Chidsey, C. E. D., Liu, G.-Y., Rowentree, P. & Scoles, G. J. *J. Chem. Phys.* **91,** 4421–4423 (1989).
8. Rappe, A. K. *et al. J. Am. Chem. Soc.* **114,** 10024–10035 (1992).
9. Weast, R. C., Astle, M. J. & Beyer, W. H. (eds) *CRC Handbook of Chemistry and Physics* 66th Edn F174–F184 (CRC Press, Boca Raton, 1986).
10. Smith, T. *Adv. Colloid Interface Sci.* **3,** 161–221 (1972).
11. De Levie, R. *Chem. Rev.* **88,** 599–609 (1988).
12. Buess-Herrman, C. *Prog. Surf. Sci.* **46,** 335–375 (1994).
13. Magnussen, O. M. *et al. Phys. Rev. Lett.* **74,** 4444–4447 (1995).
14. Barton, S. W. *et al. Nature* **321,** 685–687 (1986).
15. Regen, M. J. *et al. Phys. Rev. Lett.* **75,** 2498–2501 (1995).
16. Pershan, P. S. & Als-Nielsen, J. *Phys. Rev. Lett.* **52,** 759–762 (1984).
17. Weinbach, S. P. *et al. Adv. Mat.* **7,** 857–862 (1995).
18. Wu, X. Z. *et al. Phys. Rev. Lett.* **70,** 958–961 (1993).
19. Grübel, G., Als-Nielsen, J. & Freund, A. K. *J. de Phys. IV* **4,** 27–34 (1994).

ACKNOWLEDGEMENTS. We thank C. Chidsey for providing the C_{22} and C_{30} thiols and D. Mandler, I. Rubinstein, G. Whitesides and P. Fenter for discussions. This work was supported by the Division of Material Sciences, US Department of Energy, the US National Science Foundation, and the US–Israel Binational Science Foundation.

CORRESPONDENCE should be addressed to O.M.M. (e-mail: olaf.magnussen@chemie.uni-ulm.de).

Prediction of global rainfall probabilities using phases of the Southern Oscillation Index

Roger C. Stone, Graeme L. Hammer & Torben Marcussen

Agricultural Production Systems Research Unit, Queensland Department of Primary Industries and Commonwealth Scientific, Industrial and Research Organisation, PO Box 102, Toowoomba, Queensland, Australia 4350

THE El Niño/Southern Oscillation (ENSO) is a quasi-periodic interannual variation in global atmospheric and oceanic circulation patterns, known to be correlated with variations in the global pattern of rainfall[1–3]. Good predictive models for ENSO, if they existed, would allow accurate prediction of global rainfall variations, thus leading to better management of world agricultural production[4,5], as well as improving profits and reducing risks for farmers[6,7]. But our current ability to predict ENSO variation is limited. Here we describe a probabilistic rainfall 'forecasting' system that does not require ENSO predictive ability, but is instead based on the identification of lag-relationships between values of the Southern Oscillation Index, which provides a quantitative measure of the phase of the ENSO cycle, and future rainfall. The system provides rainfall probability distributions three to six months in advance for regions worldwide, and is simple enough to be incorporated into management systems now.

Climate forecast systems offer a means to reduce risks in potentially 'bad' years and maximize profits in potentially 'good' years. The Southern Oscillation Index (SOI) provides a measure that can be used in developing a seasonal forecast system. The SOI is here defined as the difference in atmospheric pressure anomalies between Tahiti and Darwin divided by the standard deviation of the difference (and multiplied by 10)[8]. The SOI is moderately correlated with future seasonal rainfall in some regions[9,10], partly due to the strong auto-correlation between SOI values in early austral winter with those three to six months ahead[11]. This 'phase-locking' of the SOI into the annual cycle permits seasonal forecasting to be attempted once the early stages of various manifestations of the ENSO cycle are underway. In other words,